

# HIGH PRANDTL NUMBER MIXED CONVECTION CAVITY FLOW USING LATTICE BOLTZMANN METHOD

*M.A.Taher*

*H.D.Kim*

Dept. of Mechanical Engineering, Andong National University, Korea

*Y.W.Lee*

Dept. of Mechanical Engineering, Pukyong National University, Korea

---

## Abstract

The mixed convection heat transfer and fluid flow behaviors in a lid-driven square cavity filled with high Prandtl number fluids at low Reynolds number have been studied using Thermal Lattice Boltzmann Method (TLBM). The LBM has built up on the D2Q9 model called the Lattice-BGK (Bhatnagar–Gross–Krook) model. The Lattice Boltzmann momentum and energy equations are considered simultaneously to solve the problem. Effects of non dimensional mixed convection parameter, namely buoyancy parameter or Richardson number ( $Ri$ ) in presence of heat generation ( $q$ ) with moving lid are discussed to investigate the thermal and fluid flow behaviors. It deals with continuing and comparison study of authors recent published work (Taher et al. 2013). The results are presented as velocity and temperature profiles as well as stream function and temperature contours for  $0.50 \leq Ri \leq 10.0$  and  $q$  ranging from 0.0 to 0.10 with other controlling parameters. It is found that LBM has good potential to simulate mixed convection heat transfer and fluid flow problems. The mixed convection parameter,  $Ri$ , provides an important measurement of the thermal natural convection forces relative to the mechanically induced lid-driven forced convection with heat generation ( $q$ ) effects. Moreover, it is found that the overall heat transfer rate in terms of Nusselt number ( $Nu$ ) are significantly increased with increasing  $Ri$  and decreased very slightly with increasing the values of heat generation. Finally, the simulation results have been compared with the previous numerical and experimental results and it is found to be in good agreement.

---

**Keywords:** Lattice-Boltzmann, Richardson number, lid-driven, Prandtl number, heat generation, mixed convection

## Introduction

The phenomenon of two-dimensional mixed convection in a lid-driven cavity received increasing attention because of its wide applications in engineering and science. Some of these applications include oil extraction, solar energy collector, cooling of electronic devices and heat transfer improvement in heat exchanger devices etc. It has been intensively studied last century. The lid-driven closed cavities mechanically driven by tangentially moving walls represents a basic problem in convection heat transfer. Mixed convection in cavity of various shapes with different boundary conditions and medium have been studied by many researchers (Pop et al. 2003, Hussein and Hussain, 2010). However, sometimes it is important to simulate thermal effects simultaneously with the fluid flows. Obviously, the temperature distribution in a flow field is of central interest in heat transfer problems. In most geophysical flows, the temperature difference is the driving mechanism of the motion of the fluid. From a practical point of view, the research on natural and mixed convection in a cavity has been investigated by Khanafer et al. 2003 and Krane and Jessee 1983. At the very recently, the effect of inclination angle on heat transfer rate and flow pattern inside a lid-driven square cavity with different mixed convection parameter has been studied by Darzi et al. 2011. In their study they have shown that, the rate of heat transfer and the Richardson number, mixed convection parameter are opposite because the natural convection changes to mixed convection or forced convection when Richardson number decreases. Lattice Boltzmann Method (LBM), based on Boltzmann equation (BE), is one of the methods available to deal with such kind of problems. At the recent year, this method has attracted much attention as a novel alternative to traditional methods for numerically solving the Navier–Stokes (N–S) equation (Taher and Lee 2012 and Taher et al. 2010). Lattice gas models with an appropriate choice of the lattice symmetry in fact represent numerical solutions of the Navier–Stokes equations and therefore able to describe the hydrodynamics problems have been discussed by McNamara and Zanetti 1988 and Wei et al. 2004. Due to the sampling of the particle velocities around zero velocity, LBM is limited to the low Mach number (nearly incompressible flow) flow simulation. The introduce of the LBM and gas kinetic BGK scheme in the low-Mach number viscous flow simulations have been discussed by Xu and He 2003. It is commonly recognized that the Lattice Boltzmann method (LBM) can faithfully be used to simulate the incompressible Navier–Stokes (N–S) equations with high accuracy and this lattice BGK (LBGK) model, the local equilibrium distribution has been chosen to recover the N–S macroscopic equations (Chen et al. 1992, and Qian et al. 1992). He et al. 1998 discussed more details about thermal model for the LBM in incompressible limit. In this model, the

temperature can be calculated using an internal energy distribution function, where the macroscopic density and velocity are still simulated using density distribution function. This thermal Lattice Boltzmann model (TLBM) is successfully implemented with different conditions by many researchers (Bhaumik and Lakshminisha 2007, Dixit and Babu 2006, Patil et al.2006). In addition, a thermal Lattice Bhatnagar– Gross–Krook (TLBGK) models with some adjustable parameters with Boussinesq approximation have been discussed by Taher et al.2013 and White et al.2000. The more details about TLBM with some examples for different cases have been discussed by many authors(Mohammad 2007 and Succi 2001).

The problem of mixed convection fluid flow and heat transfer analysis in a lid-driven cavity filled with different high Prandtl number fluids, mineral oil ( $Pr = 450$ ,  $\nu = 3.45 \times 10^{-5} \text{ m}^2/\text{s}$ ) and engine oil ( $Pr = 5400$ ,  $\nu = 1.2 \times 10^{-4} \text{ m}^2/\text{s}$ ) with low Reynolds number,  $Re=10$ , have been studied by using thermal Lattice Boltzmann method (TLBM). A constant heat source is placed at the mid section of the bottom cavity wall, where left and right walls are maintained at hot and cold temperature. A few investigations of mixed convection in a cavity with upper moving lid in presence of heat source on the bottom wall using TLBM, are found in the literature, but to the author's knowledge, the above mentioned problem has not been studied yet by this method. To analyze the fluid flow and heat transfer characteristics, the simultaneous effects of mixed convection and heat generation with moving lid, considering two different working fluid, have numerically been studied in the present work.

### **Formulation of the Problem**

The physical model with boundary conditions for the present study is shown in Figure1. The computational domain is to consider as a closed square cavity of length, the upper horizontal wall moves from left to right with a constant velocity, while the other three walls are fixed. The horizontal walls are assumed to be insulated whereas the vertical walls are maintained at constant but different temperatures  $T_h$  (hot) and  $T_c$  (cold). A solid block or thin heater, 10% of the total length of bottom wall, is placed at the mid section of the bottom wall.

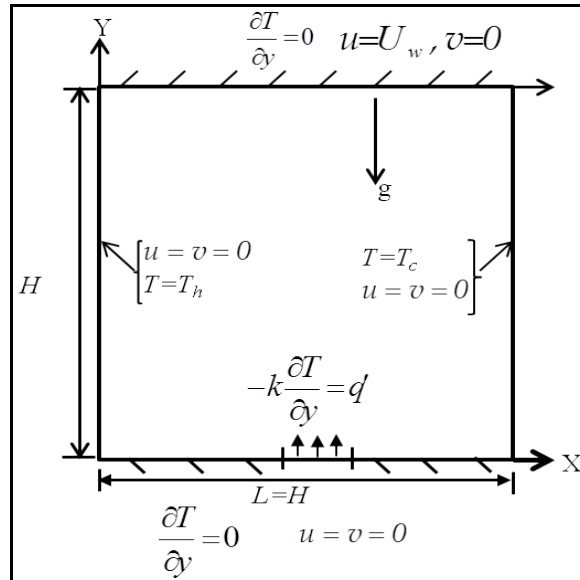


Figure 1- The configuration of the problem under consideration.

In LBM, the movement of the fluid particles is considered instead of directly solving the macroscopic fluid quantities like the velocity and the pressure. It is known as mesoscopic simulation model, which is based on the Boltzmann equation. Neglecting external forces, the Boltzmann equation (BE) with BGK approximation can be written as

$$\frac{\partial F_i}{\partial t} + e_i \cdot \frac{\partial F_i}{\partial \vec{x}_i} = -\frac{1}{\tau} (F_i - F_i^{eq}), \quad i = 0, 1, 2, \dots, n-1 \quad (1)$$

Where,  $F_i(\vec{x}, t)$  is the particle distribution function (PDF) and  $F_i^{eq}$  is the equilibrium distribution function at lattice position  $\vec{x}$  and time  $t$  discussed by Qian et al.[12]. The relaxation parameter,  $\tau$ , which is linked to the viscosity ( $\nu$ ) of the fluid. In order to solve for  $F_i$  numerically, we need to discretized the equation (1) in the velocity space using a finite set of particle velocity vectors  $\vec{e}_i, i = 0, 1, \dots, n-1$ , where  $n$  is the number of directions of the particle velocities at each node. The lattice model with particle velocity vectors ( $\vec{e}_i$ ) in D2Q9 model is shown in Fig.1.

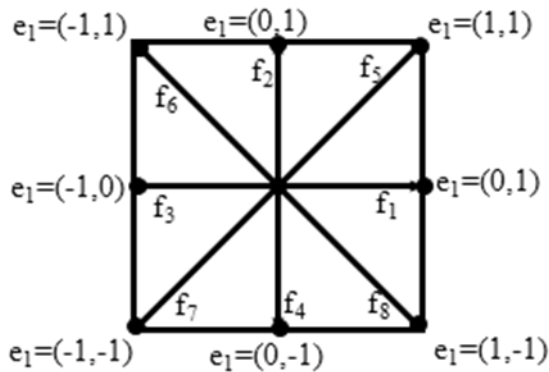


Figure 2-A D2Q9 lattice model with particle velocity vectors ( $e_i$ ).

Therefore, the discrete form of equation (1), adding force term with some adjustable coefficients, is called the Lattice Boltzmann equation (LBE) and it can be written as

$$F_i(\vec{x} + \Delta t \vec{e}_i, t + \Delta t) - F_i(\vec{x}, t) = -\frac{1}{\tau}(F_i(\vec{x}, t) - F_i^{eq}(\vec{x}, t)) + \frac{2\tau - 1}{2\tau} \frac{D}{A_i c^2} \vec{e}_i \cdot \vec{F}_a \quad (2)$$

The function  $F_i(\vec{x}, t)$  is the discrete particle distribution function and  $F_i^{eq}$  is the discrete equilibrium distribution function at lattice position  $\vec{x}$  and time  $t$  with lattice velocity vector  $\vec{e}_i$  discussed by Wei et al.2004. The last term of (2), called forced term should introduce more carefully because of high Prandtl number (Pr). Therefore, it is need to adjust some coefficient to the applied force,  $\vec{F}_a$ , e.g.  $A_i$  is the adjustable coefficient,  $D$  is the dimension. The relaxation parameter,  $\omega = 1/\tau$ , depends on the local macroscopic variables,  $\rho$  and  $\rho \vec{u}$ . These variables should satisfy the following laws of conservation:

$$\rho = \sum_i F_i \quad \text{and} \quad \rho \vec{u} = \sum_i \vec{e}_i F_i \quad (3)$$

In presence of any interaction or any external forces, the velocity should modified by the force term in calculating the equilibrium distribution

functions as  $\vec{u}^{eq} = \vec{u} + \frac{\tau \vec{F}_a}{\rho}$ . The above equations are the working horse of

the lattice Boltzmann method and replaces N-S equations in CFD by appropriate choice of lattices and  $F_i^{eq}(\vec{x}, t)$ . The form of this equilibrium distribution function must be chosen so that the fluid mass and momentum are conserved. For two dimensional D2Q9 model, the equilibrium distribution function is defined by Wei et al. 2004.

$$F_i^{eq} = \rho w_i \left[ 1 + \frac{3}{c^2} \bar{e}_i \cdot \bar{u}^{eq} + \frac{9}{2c^4} (\bar{e}_i \cdot \bar{u}^{eq})^2 - \frac{3}{2c^2} u^{eq2} \right] \quad (4)$$

Simultaneously, the lattice Boltzmann energy equation without viscous dissipation [14] can be written as

$$G_i(\bar{x} + \Delta t \bar{e}_i, t + \Delta t) - G_i(\bar{x}, t) = -\frac{1}{\tau_\theta} (G_i(\bar{x}, t) - G_i^{eq}(\bar{x}, t)) \quad (5)$$

It is noted that the internal energy,  $\varepsilon$ , is related (proportional) to the temperature by the thermodynamic relation  $\varepsilon = \sum_i G_i(x, t) = \rho c_p T$ .

Therefore, the mean temperature of the fluid in this model can be written as

$$T = \frac{\varepsilon(x, t)}{\rho c_p} = \frac{\sum_i G_i(x, t)}{\rho c_p} \quad (6)$$

The above expressions (3) and (6) describe the relationships between the microscaled quantities and the macro scaled physical quantities. Using the Chapman-Enskog expansion, it is mathematically provable that the above equations recover the N-S equation both for velocity and temperature fields (Wei et al. 2004, He et al.1998), if pressure, viscosity coefficient ( $\mu$ ) and thermal diffusivity( $\alpha$ ) are identified in lattice unit as respectively,  $P = \rho Cs^2$ ,  $\nu = \left( \tau - \frac{1}{2} \right) Cs^2$  and  $\alpha = \left( \tau_\theta - \frac{1}{2} \right) Cs^2$  respectively. Here  $Cs = \sqrt{RT}$  is the speed of sound in lattice unit. Solving the equations (1) and (6) with other approximations, we get all information that we interested in our study. It is solved on a uniform 2D grid system along with boundary conditions and other equations described as above. Each numerical time steps consists of three stages: (i) collision, (ii) streaming, and (iii) boundary conditions steps followed by the LBM approaches. More details, please the books Mohammad 2007 and Succi 2001.

### Results and Discussions

Data are obtained for two different working fluids: mineral oil and engine oil with Prandtl number approximately 450 and 5400 respectively. The viscosity,  $\nu = 3.45 \times 10^{-5} \text{ m}^2/\text{s}$ , and  $\nu = 1.2 \times 10^{-4} \text{ m}^2/\text{s}$  for the Prandtl number,  $Pr = 450$  and  $Pr = 5400$  respectively are taken with low Reynolds number,  $Re=10$ . The moving lid velocity is taken,  $U_w = 0.002$  (lattice unit) for  $Pr= 450$  and  $U_w = 0.005$  (lattice unit) for  $Pr = 5400$  to match the fixed Reynolds number ( $Re=10$ ) and the lattice nodes of the geometry. For natural convection, the momentum and energy equations are coupled and the flow is driven by temperature or mass gradient, i.e. buoyancy force. Hence there is an extra force term that needs to be considered in solving LB equations.

Under Boussinesq approximation, the force term per unit mass can be written as  $\vec{F}_a(\vec{x}, t) = \rho(\vec{x}, t) g \beta(T(\vec{x}, t) - T_{ref})$ , where  $T_{ref}$  is the reference temperature of the fluid,  $g$  is the gravitation acceleration,  $\beta$  is the thermal expansion coefficient. For small temperature difference, the buoyancy force is balanced by viscous drag and heat dissipation. The ratio of the buoyancy force to the product of viscous force and heat diffusion rates defines the

Rayleigh number,  $Ra = Pr \times Gr = \frac{g\beta\Delta TH^3}{\nu\alpha}$ , where  $Gr = \frac{g\beta\Delta TH^3}{\nu^2}$  is the

Grashof number,  $Pr = \nu/\alpha$  is the Prandtl number. The ratio  $Gr/Re^2$  is the mixed convection parameter and it is called the buoyancy parameter or

Richardson number (Ri) i.e.  $Ri = \frac{Gr}{Re^2}$ . Actually, it is a measure of the

relative strength of the natural convection to forced convection for a particular problem. Here,  $x$  and  $y$  are normalized by  $N_x$  and  $N_y$  respectively, where  $N_x$  is the lattice node in  $x$ - direction and  $N_y$  is the lattice node in  $y$ -direction. The velocity  $u$  and  $v$  by the characteristic speed  $U_0$ , where  $U_0 = \sqrt{g\beta\Delta TH}$  must be chosen carefully, so that the low Mach number approximation holds in order to insure the problem is in the incompressible regime.

### Convergence Test

In this model, there is a difficulty that it can take time to reach the stable state. Because, when the flow is induced across the lattice, it takes time for particles to distribute themselves across the lattice. This leads to fluctuations in the behavior of the flow until the model has time to settle down into a stable state. Therefore, numerical stability and iteration to converge need the particles to be at equilibrium state. In this simulations, it is depend on the number of iterations, called time steps in LBM. The number of time steps is considered until the solution is obtained at convergence criteria for the fluid flow dependent variables like velocity, pressure, temperature etc. The dimensionless U-velocity profile is shown in Figure 3 for lattice time steps up to 500000  $t_s$  (lattice unit). It is clearly seen that the flow variable converge to the steady state solutions after 120000 iterations, times steps in lattice unit. In order to get better approximations, throughout our calculations, it is considered 500000 time steps. The computations were carried out with a code developed by the authors and written in FORTRAN language.

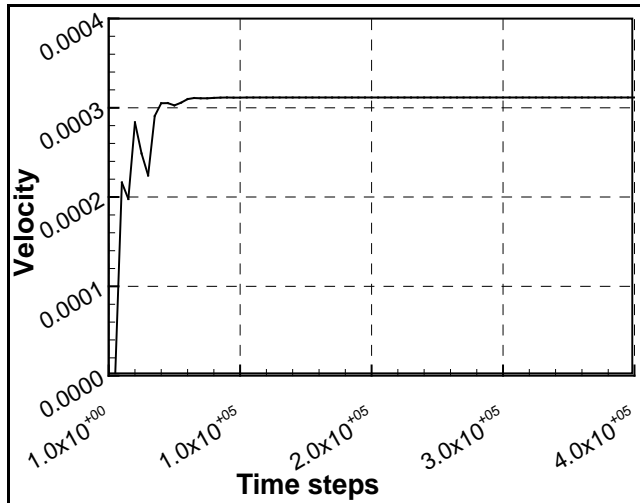


Figure 3- Convergent test: U-velocity versus lattice time steps.

### Code Validation

In order to assess the accuracy of our method, we compare our results with others published data relating to natural convection flow in a square cavity. Numerical values of dimensionless temperature at different locations of horizontal central line of the square cavity are summarized in Table-1.

**Table-1:** A comparison of dimensionless temperature,  $T$ , at the horizontal centre line of the square cavity for  $Pr = 0.71$  and  $Ra = Ra = 1.89 \times 10^5$ .

X(x/H)	Krane&Jessee[4]-Exp	Khanafer et al.[3]-Num	Present-LBM
0.13	0.522	0.483	0.497
0.30	0.496	0.490	0.485
0.50	0.528	0.493	0.491
0.70	0.532	0.501	0.495
0.80	0.539	0.515	0.504
0.90	0.465	0.452	0.481

Table-1 depicts the comparison of the present numerical results of non-dimensional temperature  $T(X, Y/2)$  for Prandtl number,  $Pr = 0.71$ , at different positions of  $X$  obtained by LBM with those experimental results obtained by Krane & Jesse 1983 and Numerical results by Khanafer et al. 2003. It is seen that the results are in good agreement with those of present authors and this confirms the accuracy of our present work. The validation for other dependent variables as well as grid independent test have been discussed more details in Taher et al.2013.

### Prandtl Number Effects

The velocity and temperature profiles have been studied for two different working fluids,  $Pr = 450$  and  $Pr = 5400$ , with various values of mixed convection parameter, Richardson number,  $Ri$ , and heat generating source are shown in Figs. 4–6. The vertical velocity component rises along the hot wall and falls along the cold wall, as expected in Fig. 4 and Fig.5. In more details, the velocity along the vertical walls of the cavity show a higher level of activity as predicted by thin layer of hydrodynamic velocity boundary layers. The locations of the local maximum and minimum velocities for all cases tend to near the walls with increasing the bouyancy parameter, namely the Richardson number,  $Ri$ , are shown in Fig. 5. However, these location slightly moves toward the center of the cavity in presence of heat generation effect.

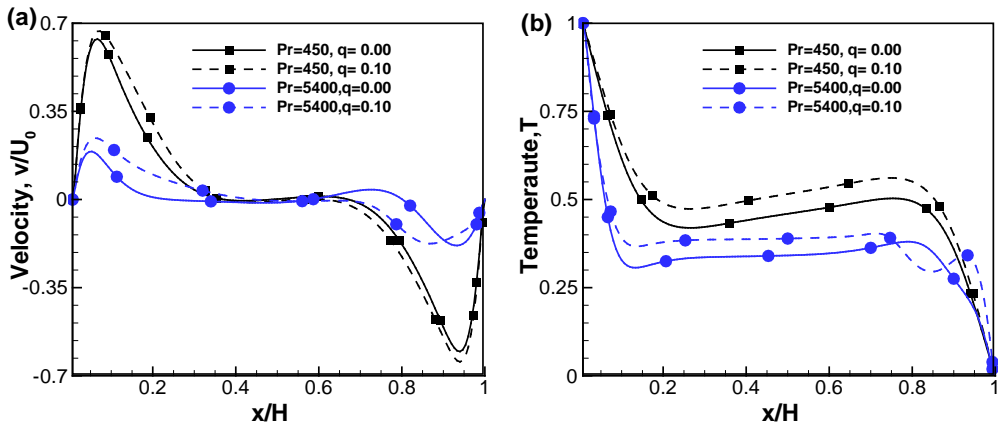


Figure 4- (a) Dimensionless V-velocity and (b) temperature profiles along horizontal centreline of the cavity for  $q = 0.0$  and  $0.1$  with  $Pr = 450$  and  $5400$ .

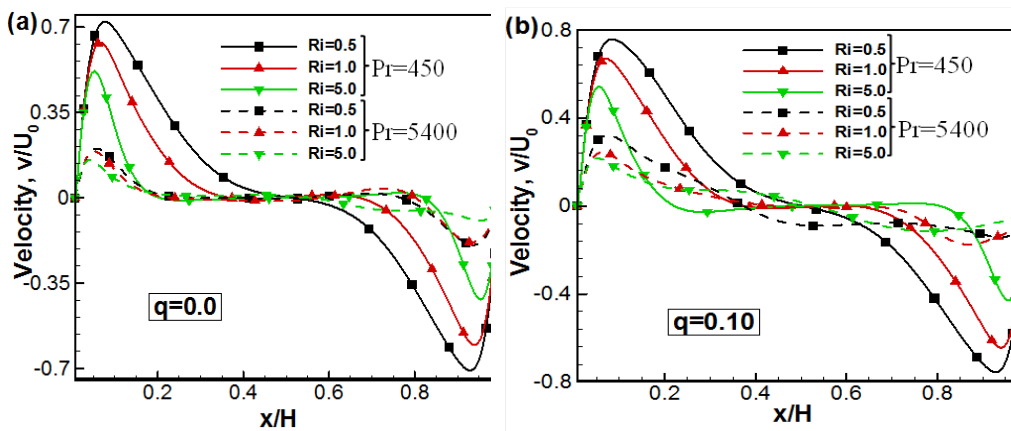
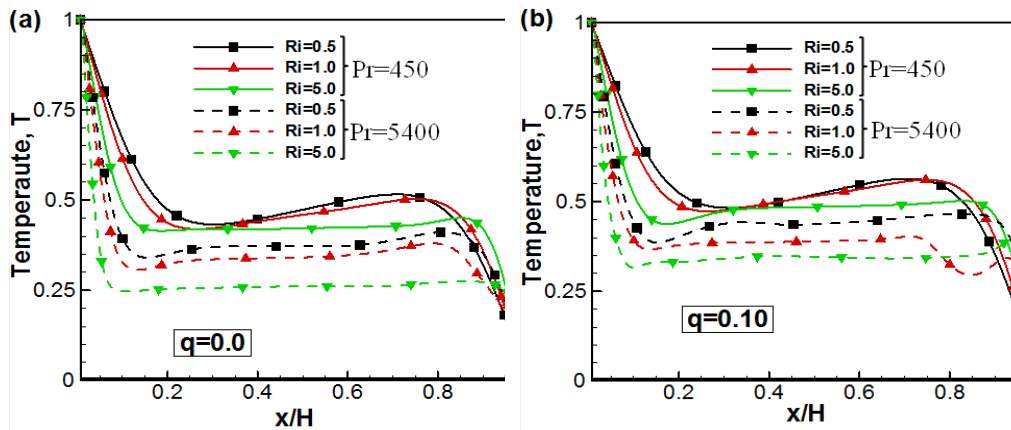


Figure 5 - Dimensionless V-velocity profiles along horizontal centreline of the cavity for different values of  $Ri$  ( $=0.05, 1.0, 2.0$  and  $5.0$ ) and Prandtl numbers ( $Pr = 450$  and  $5400$ ) (a) with no generation (b) with heat generation.



**Figure 6- Dimensionless temperature profiles along horizontal centreline for different values of  $Ri$  ( $= 0.05, 1.0, 2.0$  and  $5.0$ ) and Prandtl numbers  $Pr$  ( $=450$  and  $5400$ ) (a) with no generation and (b) with heat generation.**

The effect of dimensionless temperature profiles with different values of mixed convection parameter,  $Ri$ , at the centreline of the cavity are shown in Fig.6. The variation of temperature near hot and cold walls versus dimensionless horizontal length is linear for all  $Ri$ , which is the characteristic of heat transfer by convection. A significant temperature gradient is observed in the vicinity of the heated and cold walls approximately,  $0 \leq X \leq 0.3$ , and  $0.75 \leq X \leq 1$  respectively for  $Ri=0.5$  and  $Pr = 450$ . Therefore, the core region in this case is seen approximately  $0.3 < X < 0.75$ . The core region is increased with increasing the mixed convection parameter  $Ri$  as well as Prandtl number. In physical meaning, the temperature should decrease in the increase of  $Ri$ . It means that the natural convection is dominant compare to forced convection. This is because the upper wall is moving with constant velocity from left to right and therefore the fluid motion increases the rate of heat transfer. As a result, with the effect of moving lid, in presence of heat generation, the disturbance temperature profiles near the cold are observed in Fig. 6(b), dashed lines (red color) and in Fig. 4(b), dashed line with circle, for very high Prandtl number working fluid. These types of fluid flow and heat transfer are explained more details in the author recent published paper Taher et al.2013.

### Mixed Convection and Heat Generation Effects

In the above section, it has been discussed the effects of Prandtl number, so in this section we will discuss the mixed convection as well as heat generation effects on fluid flow and heat transfer analysis by considering  $Pr=450$ . For similar cases for  $Pr=5400$ , the details are discussed in same author published work mentioned as above.

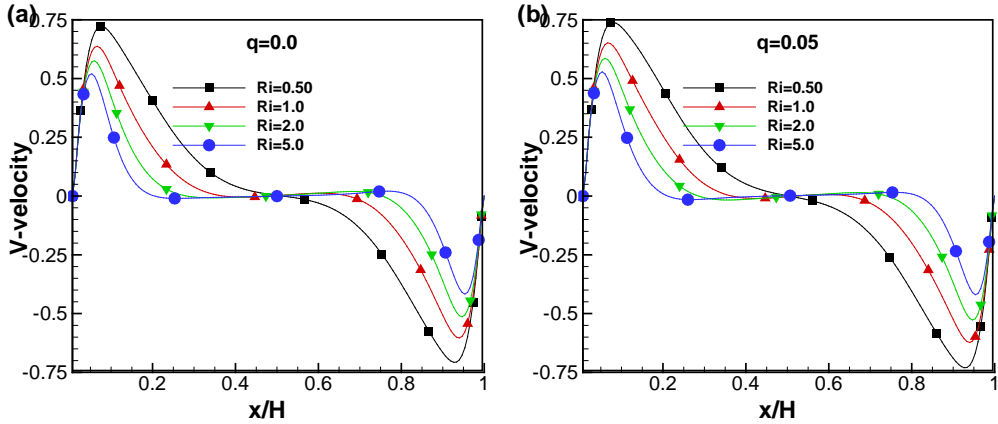


Figure 7- V-velocity profiles along horizontal centreline of the cavity for different values of buoyancy parameter, Ri (a) with no generation and (b) with heat generation.

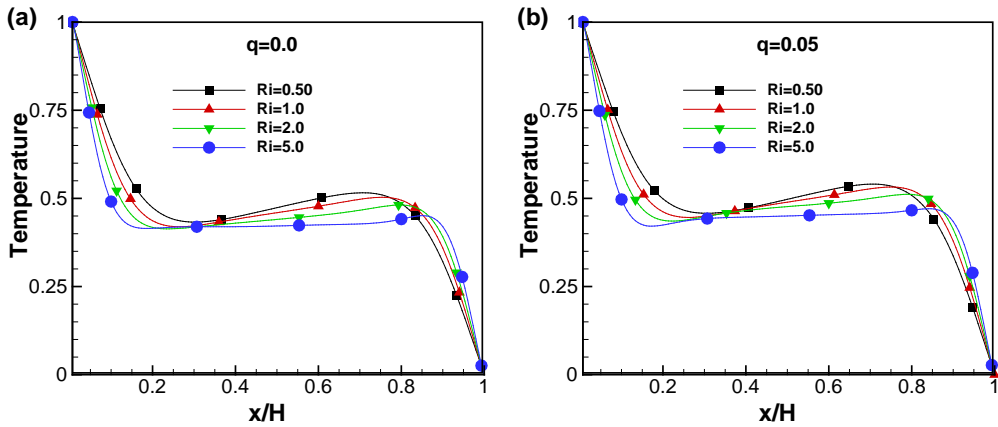


Figure 8- Dimensionless temperature profiles along horizontal centreline for different values of buoyancy parameter, Ri (a) with no generation and (b) with heat generation.

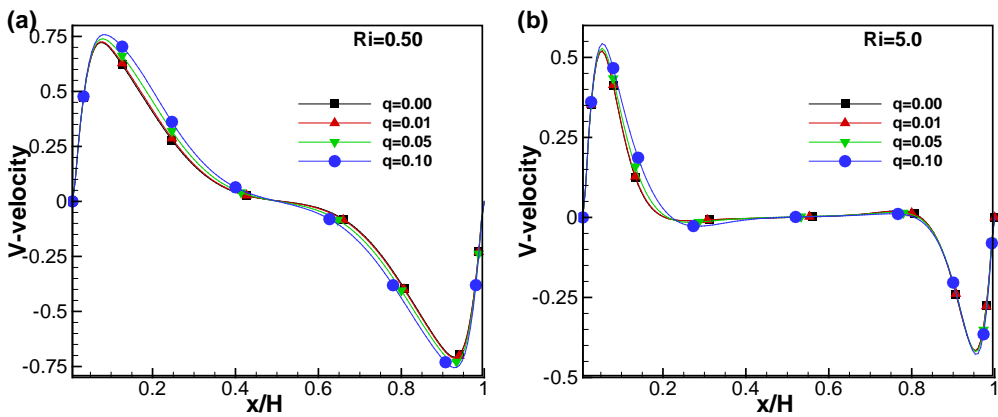
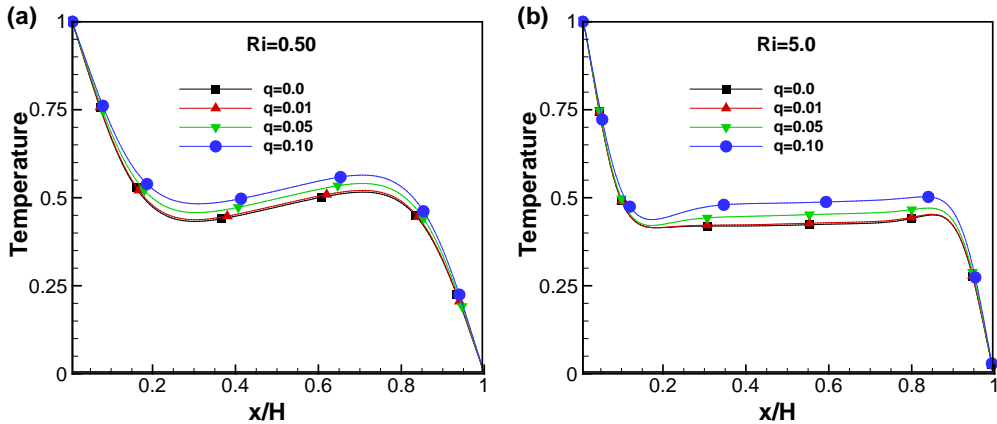
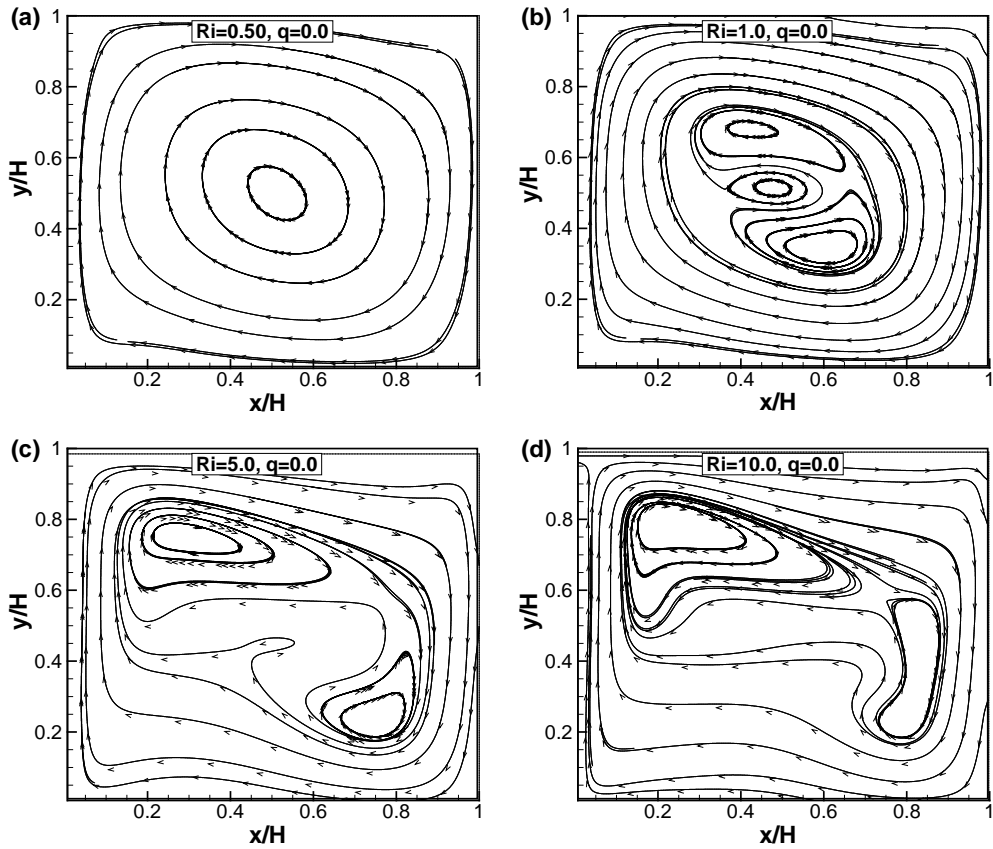


Figure 9- Dimensionless V-velocity profiles along horizontal centreline of the cavity for different values of  $q$  with buoyancy parameter (a)  $Ri=0.5$  and (b)  $Ri=5.0$ .

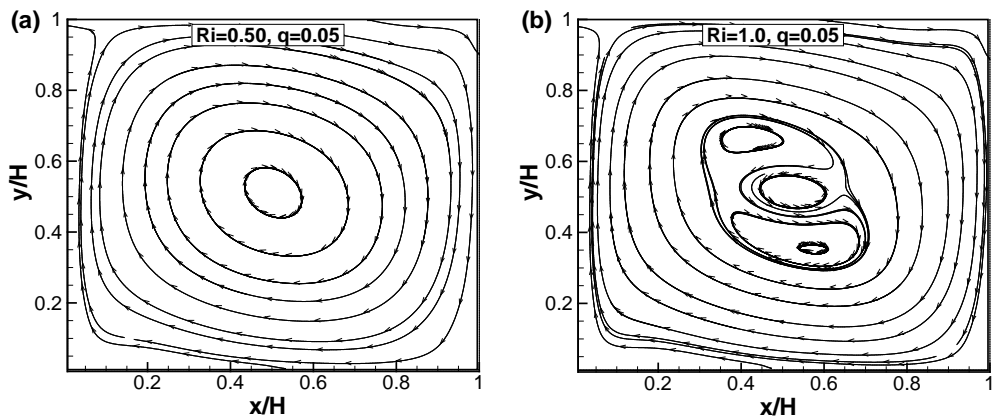


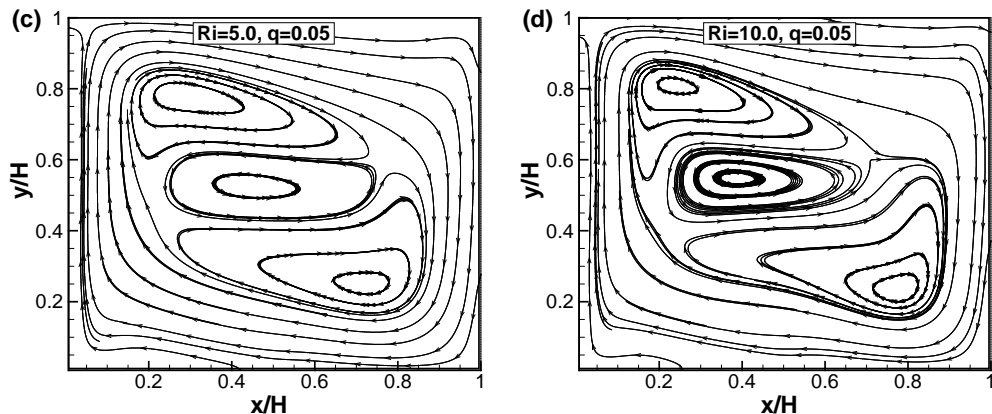
**Figure 10- Dimensionless temperature profiles along horizontal centreline of the cavity for different values of  $q$  with buoyancy parameter (a)  $Ri=0.5$  and (b)  $Ri=5.0$ .**

Figures 7 and 8 described the dimensionless V-velocity and temperature along the horizontal centreline for different values dimensionless mixed convection parameter or buoyancy parameter called Richardson number,  $Ri$ , ranging from 0.5 to 5.0 with in presence of heat generation and without heat generation effect as well. It is seen that with increasing the buoyancy effect, the local maximum and minimum shifted to near the walls. Therefore, the core region at the center of the cavity increases. Consequently, the similar phenomeon are observed for the dimensinless temperature. It may concluded that both thermal and hydrodynamic boundary layer thickness decreases significantly with increasing the mixed convection parameter  $Ri$  for  $Pr=450$ . In addition, for  $Pr=5400$ , this boundary layers become more thinner then compare to  $Pr=450$ . Moreover, from Figs. 9-10, it is seen that both of velocity boundary layer and thermal boundary layer thickness are increased very slightly with increasing the values of heat generation withing the range from 0.0 to 0.10. This is because of thermal stratification and increased the temperature in the direction of heat flow in the core region of the cavity. For better understanding the fluid flow and heat transfer analysis, the temperature and streamlines contours are illustrated in Figs. 11-14 for different non dimensional mixed convection parameter in presence of heat generation and without heat generation.



**Figure 11- Streams lines contours for different values of mixed convection parameter(Ri = 0.50, 1.0, 2.0 and 5.0) without heat generation effect.**

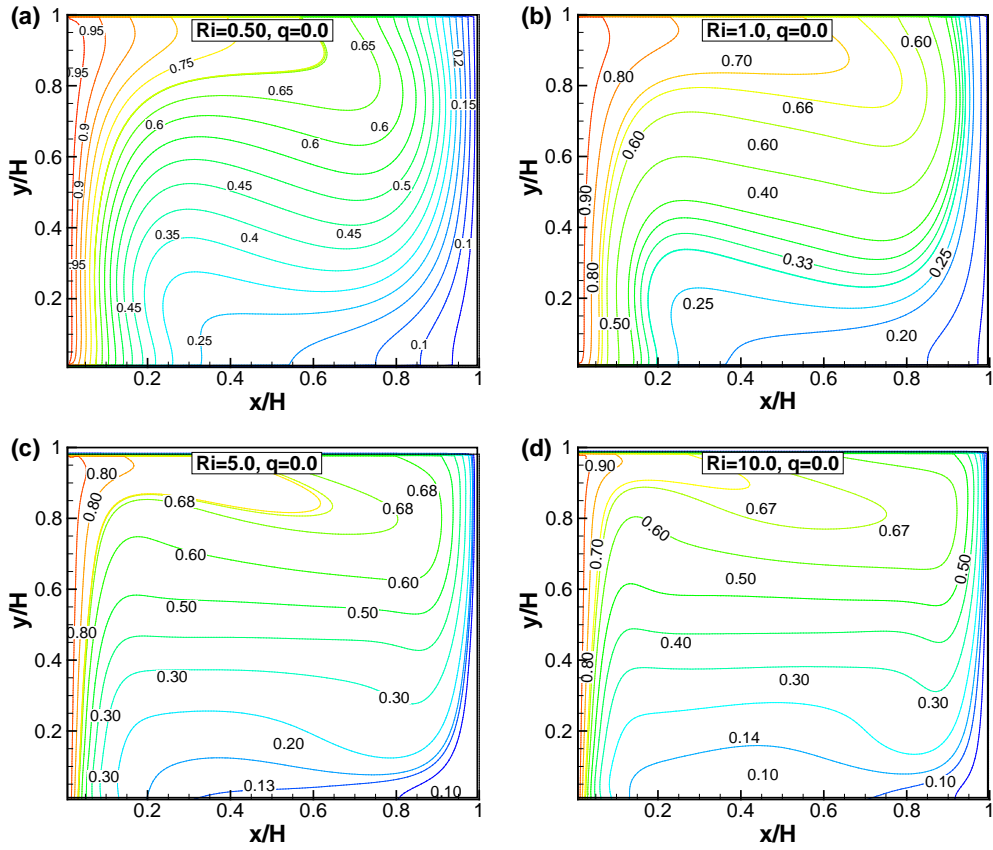




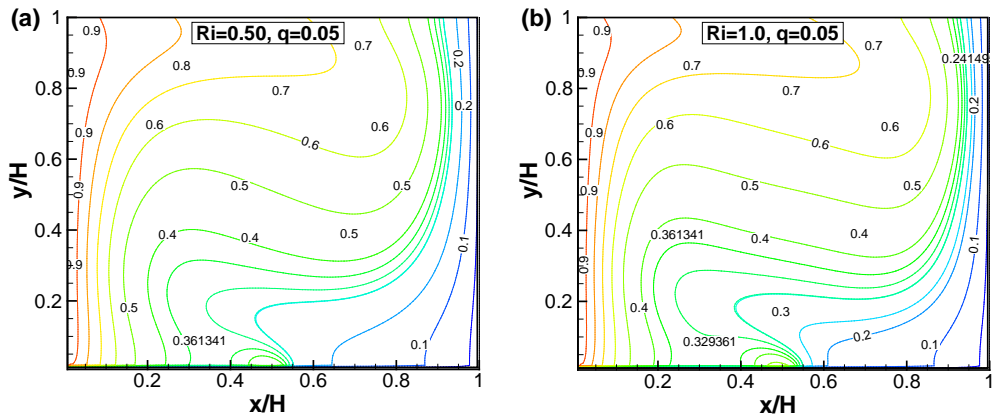
**Figure 12- Streamlines contours for different values of mixed convection parameter ( $Ri = 0.50, 1.0, 2.0$  and  $5.0$ ) in presence of heat generation.**

The streamlines for different values of non dimensional mixed convection parameter with heat generation and without heat generation are shown in Figures 11–12. Both in absence and presence of heat generation, a recirculation zone at the center of the cavity, are observed in Fig.11(a) and 12 (a) for  $Ri < 1.0$ . However, increasing the buoyancy effect,  $Ri \geq 1$ , the size and shape of central vortex has been changed and tend to become a skew-symmetry (Fig.11-(d)) in absence of heat generation because the natural convection becomes dominant with the increasing of  $Ri$ . However, in presence of heat generation, one anticlockwise vortex is seen at the center of the cavity and simultaneously two clockwise vortices are seen withing the range of  $1.0 \leq Ri \leq 10.0$  due to the combined effect of moving lid and heat generation with buoyancy parameter. Further ioncreased, not seen in the fig., the flow properties become skew symmetry, which is one of the main criteria of natural convection in a cavity.

Figures 13–14, the temperature contours have been illustrated for different values of non-dimensional mixed convection parameter,  $Ri = 0.5$  to  $10.0$  as well as for different values of heat generation ranging from  $0.0$  to  $0.10$  respectively.



**Figure 13- Temperature contours for different values of mixed convection parameter ( $Ri = 0.50, 1.0, 2.0$  and  $5.0$ ) without heat generation effect.**



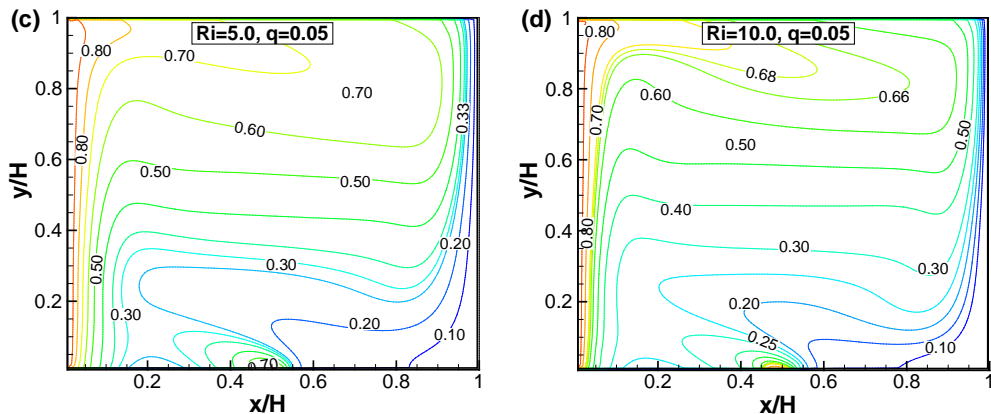


**Figure 14-Temperature contours for different values of mixed convection parameter ( $Ri = 0.50, 1.0, 2.0$  and  $5.0$ ) in presence of heat generation.**

It is seen from the above figures the heat transfer profiles changed significantly with increasing the buoyancy parameter namely the dimensionless Richardson number  $0.50 \leq Ri \leq 10$ , however, this change is not significant with increasing heat generation parameter within the range from 0.0 to 0.10. The similar phenomenon is observed in Fig.10. For  $Ri < 1.0$ , the heat is transferred mainly by forced convection between the hot and cold walls, but in presence of heat generation with moving lid, the temperature contours inside the cavity cannot significantly change due to moving lid effect. For  $Ri \geq 1.0$ , the natural convection dominates forced convection. Both in absence or presence of heat generation, buoyancy force significantly enhances the temperature contours. It is clearly seen that, owing to increasing the heat generation, the fluid temperature exceeds the surface temperature that negates the heat transfer from the heated surface. Therefore, the temperature tends to concentrate at the right vertical cold wall with increasing  $Ri$  and heat generation. Thermal boundary layer formation is also observed near the hot and cold wall. This means that heat transfer reduces when forced convection is dominated due to the presence of heat generation and moving lid.

### Heat Transfer Performance

A usual means of characterizing heat transfer is to calculate the Nusselt number. Actually, the Nusselt number,  $Nu$ , is a dimensionless form of the heat transfer coefficient. To investigate the heat transfer performance in terms of effective thermal conductivity of the fluid, the local Nusselt number,  $Nu_x$ , is calculated by  $Nu_x = \frac{\partial T}{\partial x}$ . Here  $T$  stands for non-dimensional temperature. Therefore, the average Nusselt number is calculated

as:  $Nu = \frac{1}{H} \sum_{k=1}^H \frac{\partial T}{\partial x}$ , where,  $H$  is the total number of lattice in  $y$ -direction.

The average rate of heat transfer,  $Nu$ , at the left heated wall for different values of mixed convection parameters ( $Ri = 0.05, 1.0, 2.0, 5.0$  and  $10.0$ ) in presence of heat generation are displayed in Fig.15.

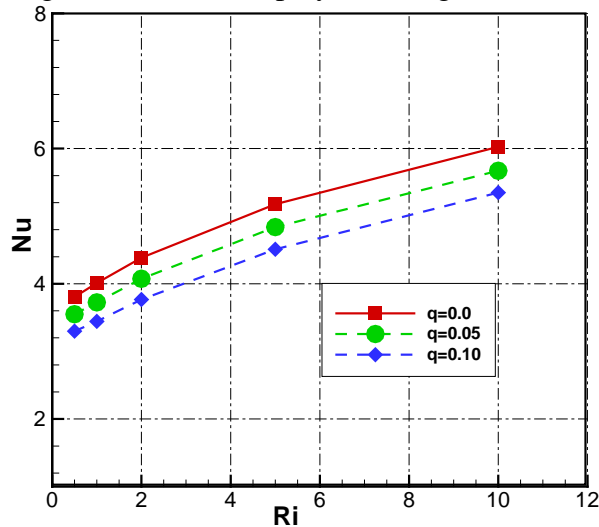


**Figure 15- Average rate of heat transfer,  $Nu$ , against mixed convection parameter ( $Ri$ ) with  $Pr=450$  for  $q=0.0, 0.05$  and  $0.10$ .**

It is seen that the rate of heat transfer linearly increased with increasing the mixed convection parameter,  $0.5 \leq Ri \leq 10.0$ . However, the heat transfer rate decreased due to in presence of heat generation at the bottom wall. This is because the fluid ambient temperature increases due to the influenced of heat generation and consequently the rate of heat transfer from left wall decreases. This decreasing rate 13.27%, 14.13%, 14.09%, 12.87% and 11.23% respectively for  $Ri = 0.05, 1.0, 2.0, 5.0$  and  $10$  with the increasing of heat generation from  $0.0$  to  $0.10$ . Actually, this rate of heat transfer depends on different boundary conditions as well as different working fluids having different Prandtl numbers. Moreover, it is seen from Taher et al.2013, that for  $Pr = 5400$ , the values of heat transfer rate is higher than that of  $Pr = 450$ . These temperature characteristics enhancement plays a significant role in engineering applications specially for electronic cooling industries or MEMS devices.

## Conclusion

Heat transfer and fluid flow analysis of high Prandtl numbers with low Reynolds number in a lid-driven square cavity have successfully been investigated using D2Q9-TLBGK model with some adjustable parameter as well as forcing terms. In this study, the mixed convection parameter ( $Ri$ )

provides an important measurement of the thermal natural convection forces relative to the mechanically induced lid-driven forced convection with heat generation ( $q$ ) effects. The present results are noted that the velocity and temperature profiles are significantly changed with increasing the mixed convection parameter,  $0.5 \leq Ri \leq 10.0$  both in present and without present of heat generation. The thickness of the velocity boundary layer and thermal boundary layer are significantly decreased, become thinner, with increasing the bouyancy paremeter. However, with increasing the values of heat generation from 0.0 to 0.10, both the velocity and thermal boundary layer thickness are increased very slightly. In addition, it is observed that both velocity and temperature boundary layer thickness decreased for very high prandtl number,  $Pr = 5400$  compare to  $Pr = 450$ . Therefore, the average rate of heat transfer interms of dimensionless Nusselt number,  $Nu$ , linearly increased with increasing mixed convection parameter in the absence of heat generation effect. However, the heat tranfer rate decreased due to increase the heat generation, the fluid temperature exceeds the surface temperature that negates the heat transfer from the heated surface. This temperature characteristics enhancement plays an important role in many engineering applications.

## Nomenclature

$c$	Courant–Friedriehs–Lewy number	
$C_s$	Lattice speed of sound	
$e_i$	Discrete particle velocity vector	[m/s]
$F_a$	Force per unit mass	[kg.m/s <sup>2</sup> ]
$F_i^{eq}$	Particle equilibrium distribution function	
$F_i$	Discrete particle distribution function	
$Gr$	Grashof number	
$G_i$	Discrete energy distribution function	
$G_i^{eq}$	Discrete energy equilibrium distribution function	
$H$	Cavity height	[m]
$k$	Thermal conductivity	[w/m.K]
$Nu$	Nusselt number	
$Pr$	Prandtl number	
$q$	Non dimensional heat generation	
$Re$	Reynolds number	
$Ra$	Rayleigh number	
$Ri$	Bouyancy parameter (mixed convection parameter)	
$T$	Non dimensional temperature	
$ts$	Lattice timestep	
$U, V$	Normalized fluid velocity in $x$ and $y$ directions	
$u, v$	Fluid velocity in $x$ and $y$ directions	[m/s]
$w_i$	Weighting factor	
$X, Y$	Normalized length in $x$ and $y$ directions	

**Greek symbols**

$\alpha$	Thermal diffusivity	[m <sup>2</sup> /s]
$\beta$	The coefficient of thermal expansion	[1/K]
$\tau$	Relaxation parameter for momentum	
$\tau_\theta$	Relaxation parameter for energy	
$\rho$	Density of the fluid	[kg/m <sup>3</sup> ]
$\mu$	Viscosity of the fluid	[kg/m. s]
$\nu$	Kinematic viscosity	[m <sup>2</sup> /s]

**References:**

Pop, I., Lesnic, D. and Ingham, D. B.: Conjugate mixed convection on a vertical surface in a porous medium. *Int. J. Heat Mass transfer*, vol.38(8), 1517–1525, 2003.

Hussein, A. K., and Hussain, S. H.: Mixed convection through a lid-driven square cavity with hot a wavy wall. *Int. J. Mechanical and Materials Engineering*, vol. 5(2), 222–235. 2010.

Khanafer, K., Vafai, K. and Lightstone, M.: Buoyancy- driven heat transfer enhancement in a two-dimensional enclosure utilizing nanofluids. *Int. J. Heat and Mass Transfer*, vol. 46, 3639–3653, 2003.

Krane ,R.J. and Jessee, J.: Some detailed field measurement for a natural convection flow in a vertical square enclosure. *Proceedings of the first ASME-JSME thermal engineering joint conference , Japan*, vol. 1, 323–329, 1983.

Darzi, A.A.R., Farhadi, M., Sedighi, K., Fattahi, E. and Nemati, H.: Mixed convection simulation on inclined lid driven cavity using Lattice Boltzmann method. *IJST, Transactions of Mechanical Engineering*, vol. 35(M1), 73–83, 2011.

Taher, M.A. and Lee ,Y.W. :Numerical study on reduction of fluid forces acting on a circular cylinder with different control bodies using Lattice-Boltzmann method. *Int. J. Energy and Technology*, vol. 4(18), 1-7, 2012.

Taher, M.A., Kui-Ming Li and Lee, Y.W.: Numerical study of H2O-Cu nanofluid using Lattice-Boltzmann method. *J. Korean Society of Marine Engineering*, vol. 34(1), 53-61, 2010.

McNamara, G.R. and Zanetti, G.: Use of the Boltzmann equation to simulate lattice-gas automata. *Physical Review Letters*, vol. 61, 2332–2335, 1988.

Wei, X., Mueller, K. and Kaufman, A. E.: The lattice Boltzmann method for simulating gaseous Phenomena. *IEEE Transactions on Visualization and computers Graphics*, vol.10(2), 164–176, 2004.

Xu, K. and He, X.: Lattice-Boltzmann method and gas kinetic BGK scheme in the low-Mach number viscous flow simulations. *J. Computational Physics*, vol.190, 100–117, 2003.

- Chen, H., Chen, S. and Matthaeus ,W.H.: Recovery of the Navier-Stokes equations using a lattice-gas Boltzmann method. *Physical Review A*, vol. 45(8), 5339–5342, 1992.
- Qian, Y. H., D’Humières, D. and Lallemand, P.: Lattice BGK models for Navier-Stokes equation. *Euro physics letter*, vol.17(6), 479 – 484, 1992.
- He, X., Chen, S. and Doolen, G.D.: A novel thermal model for the Lattice Boltzmann method in incompressible limit. *J. comp. Physics*,vol.146, 282–300, 1998.
- Bhaumik, S.K. and Lakshmisha, K.N.: Lattice Boltzmann simulation of lid-driven swirling flow in confined cylindrical cavity. *Computers and Fluids*, vol. 36, 1163–1173, 2007.
- Dixit, H.N. and Babu, V.: Simulation of high Rayleigh number natural convection in a square cavity using the lattice Boltzmann method. *Int. J. Heat and Mass Transfer*, vol.49, 727–739, 2006.
- Patil, D.V., Lakshmisha, K.N. and Rogg, B.: Lattice Boltzmann simulation of lid-driven flow in deep cavities. *Computers and Fluids*, vol. 35, 1116–1125, 2006.
- Taher, M. A., Saha, S.C., Lee, Y.W. and Kim, H.D.: Numerical study of Lid-driven square cavity with heat generation using LBM. *American J. Fluid Dynamics*, vol. 3(2), 40-47, 2013.
- White, D.M., Halliday, I., Care, C. M., Stevens. A. and Thompson, A.: An enhanced lattice Bhatnagar-Gross-Krook method for Boussinesq flow. *Physica D*, vol. 141, 199–213, 2000.
- Mohammad, A. A.: Applied lattice Boltzmann method for Transport phenomena, momentum, heat and mass transfer. The University of Calgary, Alberta, Canada, 2007.
- Succi S.: The lattice Boltzmann equation for fluid dynamics and beyond. Oxford University, UK, 2001.